Universal Signatures of Quantum Critical Points from Finite-Size Torus Spectra: A Window into the Operator Content of Higher-Dimensional Conformal Field Theories

Michael Schuler,[1] Seth Whitsitt,[2] Louis-Paul Henry,[1] Subir Sachdev,[2,3] and Andreas M. Läuchli[1]
[1]*Institut für Theoretische Physik, Universität Innsbruck, A-6020 Innsbruck, Austria*
[2]*Department of Physics, Harvard University, Cambridge, Massachusetts 02138, USA*
[3]*Perimeter Institute for Theoretical Physics, Waterloo, Ontario N2L 2Y5, Canada*
(Received 24 March 2016; revised manuscript received 3 October 2016; published 16 November 2016)

The low-energy spectra of many body systems on a torus, of finite size L, are well understood in magnetically ordered and gapped topological phases. However, the spectra at quantum critical points separating such phases are largely unexplored for $(2+1)$D systems. Using a combination of analytical and numerical techniques, we accurately calculate and analyze the low-energy torus spectrum at an Ising critical point which provides a universal fingerprint of the underlying quantum field theory, with the energy levels given by universal numbers times $1/L$. We highlight the implications of a neighboring topological phase on the spectrum by studying the Ising* transition (i.e. the transition between a Z_2 topological phase and a trivial paramagnet), in the example of the toric code in a longitudinal field, and advocate a phenomenological picture that provides qualitative insight into the operator content of the critical field theory.

DOI: 10.1103/PhysRevLett.117.210401

Introduction.—Quantum critical points continue to attract tremendous attention in condensed matter, statistical mechanics, and quantum field theory alike. Recent highlights include the discovery of quantum critical points which lie beyond the Ginzburg-Landau paradigm [1,2], the striking success of the conformal bootstrap program for Wilson-Fisher fixed points [3], and the intimate connection between entanglement quantities and universal data of the critical quantum field theory [4–8].

A surprisingly little explored aspect in this regard is the finite (spatial) volume spectrum on numerically easily accessible geometries, such as the Hamiltonian spectrum on a 2D spatial torus at the quantum critical point [9]. In the realm of $(1+1)$D conformal critical points there exists a celebrated mapping between the spectrum of scaling dimensions of the field theory in $\mathbb{R}^2$ and the Hamiltonian spectrum on a circle (space-time cylinder: $S^1 \times \mathbb{R}$) [10]. This result is routinely used to perform accurate numerical spectroscopy of conformal critical points using a variety of numerical methods [11,12]. In higher dimensions the situation is less favorable: Cardy has shown [13] that the corresponding conformal map can be generalized to a map between $\mathbb{R}^d$ and $S^{d-1} \times \mathbb{R}$. While numerical simulations in this so-called *radial quantization* geometry have been attempted at several occasions [14–18], this numerical approach remains very challenging due to the curved geometry, which is inherently difficult to regularize in numerical simulations.

Although low-energy spectra on different toroidal configurations have been discussed in the context of some specific field theories (in Euclidean spacetime) [19–23], our understanding of critical energy spectra is rather limited beyond free theories [24–28]. This is due to the absence of a known relation between the scaling dimensions of the field theory and the torus energy spectra.

In this Letter we present a combined numerical and analytical study of the Hamiltonian torus energy spectrum of the 3D Ising conformal field theory (CFT), and show that it is accessible with finite lattice studies and proper finite-size scaling. Torus energy spectra provide a universal fingerprint of the quantum field theory governing the critical point and depend only on the universality class of the transition and on the shape and boundary conditions of the torus, which acts as an infrared (IR) cutoff (but not on the lattice discretization, i.e., the ultraviolet cutoff). We will explicitly demonstrate this here for the Ising CFT. This approach will also be valuable as a new numerical tool to investigate and discriminate quantum critical points.

We provide a quantitative analysis of many low-lying energy levels of the standard $\mathbb{Z}_2$-symmetry breaking phase transition in the 3D Ising universality class. We also advocate a phenomenological picture that provides qualitative insight into the operator content of the critical point. As an application, we reveal that the torus energy spectrum of the confinement transition between the $\mathbb{Z}_2$ topological ordered phase and the trivial (confined) phase of the toric code (TC) in a longitudinal magnetic field can be understood as a specific combination of a subset of the fields and several boundary conditions of the standard 3D Ising universality class. Since the operator content of the partition function at criticality obviously differs from the standard 3D Ising universality class, we term this transition a 3D Ising* transition [29–31].

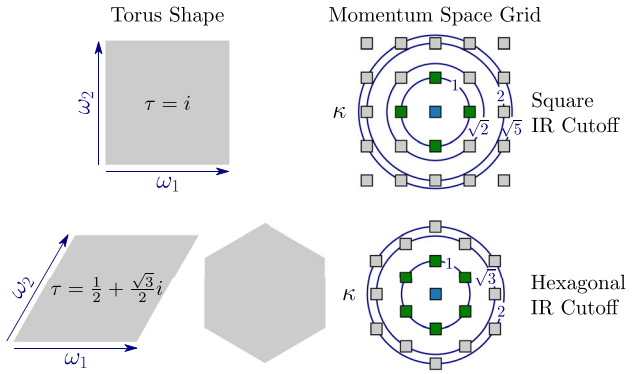

FIG. 1. The two torus geometries with fourfold and sixfold rotation symmetry and their momentum-space grid in the vicinity of the $\Gamma = (0,0)$ point. In the center of the lower row we display the Wigner-Seitz cell of the torus, highlighting the sixfold symmetry. The momentum space variable κ is defined as $\kappa = (L/2\pi)|\mathbf{k}|\tau_2$ with $\tau = \tau_1 + i\tau_2$, $L = |\omega_1| = |\omega_2|$ and $\mathbf{k}$ a momentum of the finite-size cluster.

3D Ising universality class.—In order to demonstrate the universal nature of the low-energy spectrum we study the $(2+1)$D transverse field Ising (TFI) model

$$H_{\mathrm{TFI}} = -J\sum_{\langle i,j\rangle}\sigma_i^z\sigma_j^z - h\sum_i \sigma_i^x \qquad (1)$$

on five different two-dimensional Archimedian lattices [32(a)] at their respective quantum critical point [38,39]. In our finite size simulations the spatial setup is a torus whose linear extents are determined by two spanning vectors ω_1 and ω_2 (c.f. left part of Fig. 1). The finite area leads to a discrete momentum space (c.f. right part of Fig. 1) and is equivalent to an infrared cutoff in the field theory. The use of a lattice model, on the other hand, leads to an ultraviolet (UV) cutoff in the form of a Brillouin zone. In the following we will only consider tori with $L = |\omega_1| = |\omega_2|$ and two different choices of the modular parameter $\tau = \omega_2/\omega_1$: $\tau = i$ ($\tau = 1/2 + \sqrt{3}/2i$) corresponding to a square (hexagonal) symmetry. The square and square-octagon (triangular, honeycomb, and kagome) lattices are simulated using a square (hexagonal) IR-cutoff geometry to preserve the microscopic $C_4(C_6)$ point group symmetry in the IR.

In a first step we have calculated the low-energy spectrum of the Hamiltonian Eq. (1) using exact diagonalization (ED) in all symmetry sectors on finite samples with up to $N = 40$ spins in total. The spectrum can be divided into $\mathbb{Z}_2$ even and odd sectors (spin-flip symmetry), combined with irreducible representations of the lattice space group. In the paramagnetic phase at large h/J one finds a unique $\mathbb{Z}_2$ even ground state in the fully symmetric spatial representation, with a finite gap above the ground state. At small h/J one finds two quasidegenerate ground states in the $\mathbb{Z}_2$ even and odd sector, respectively (both in the symmetric spatial representation), again with a finite gap above the ground state. At the quantum critical point $(h/J)_c$, however, the low-lying spectrum collapses as $1/\sqrt{N} \sim 1/L$, i.e., it exhibits a mass spectrum with the mass scale set by the IR cutoff. To eliminate this scaling we will multiply the excitation gaps with $\sqrt{N}$ in the following and will call that the spectrum. In Fig. 2 we display the finite size spectra at the Ising critical point for all five different lattices in the zero-momentum sector $\Gamma = (0,0)$, as well as the first momentum away from the Γ point ($\kappa = 1$ in the right part of Fig. 1). Since the speed of light is not known at this stage, the spectrum for each lattice has been globally rescaled such that the extrapolated energy of the first excited level (which is $\mathbb{Z}_2$ odd and spatially symmetric) is set to one. One explicitly observes that the critical energy spectra of lattices with the same type of IR cutoff τ (the two leftmost panels and the three rightmost panels) agree to rather high precision with each other, when taking $1/N$ finite-size corrections into account [32(b)]. This means that—as is generally expected from a field theory point of view—the obtained critical energy spectra indeed do not depend on the chosen UV discretization. In order to corroborate the extrapolations based on ED we performed extensive quantum Monte Carlo (QMC) simulations [38] of the transverse field Ising model at the critical point for all five lattices. Based on imaginary time spin-spin correlations it is possible to access the finite size gaps on lattices up to $N = 30 \times 30$ lattice sites [32(c)]. These data points (red small filled circles) in Fig. 2 reproduce the ED data where available, and allow us to confirm and sharpen the precision of the extrapolated energy spectrum. Based on the quantum numbers of the first few low-lying energy levels we choose to label them as torus analogs of the spectrum of scaling dimensions of the 3D Ising CFT: σ_T and σ_T' refer to the first two levels in the $\mathbb{Z}_2$ odd sector in the spatially symmetric representation, while ϵ_T is the first excited state (above the vacuum 1) in the $\mathbb{Z}_2$ even and spatially symmetric sector. The "$\cdots + \Delta\kappa$" label refers to levels at the first momentum away from the Γ point, $\kappa = 1$. These levels are fourfold degenerate on the square torus, while they are sixfold degenerate for the hexagonal torus. Although there is no known relation between the torus spectrum and the scaling dimensions in flat space, this phenomenological approach shows a qualitatively similar structure as the operator content of the quantum field theory.

ϵ expansion.—We also compute the energy levels using ϵ expansion. Our starting point is ϕ^4 theory, which we define by the Hamiltonian density

$$\mathcal{H} = \int d^d x \left[\frac{1}{2}\Pi^2 + \frac{1}{2}(\nabla\phi)^2 + \frac{s}{2}\phi^2 + \frac{u}{4!}\phi^4\right] \qquad (2)$$

in d dimensions with the equal-time commutator $[\phi(x,t), \Pi(x',t)] = i\delta^d(x-x')$, and specialize to the critical point, $s = s_c$, $u = u^*$. We generalize the two-dimensional torus to arbitrary dimension by taking $d/2$ copies of the desired tori in Fig. 1, so that all spatial point

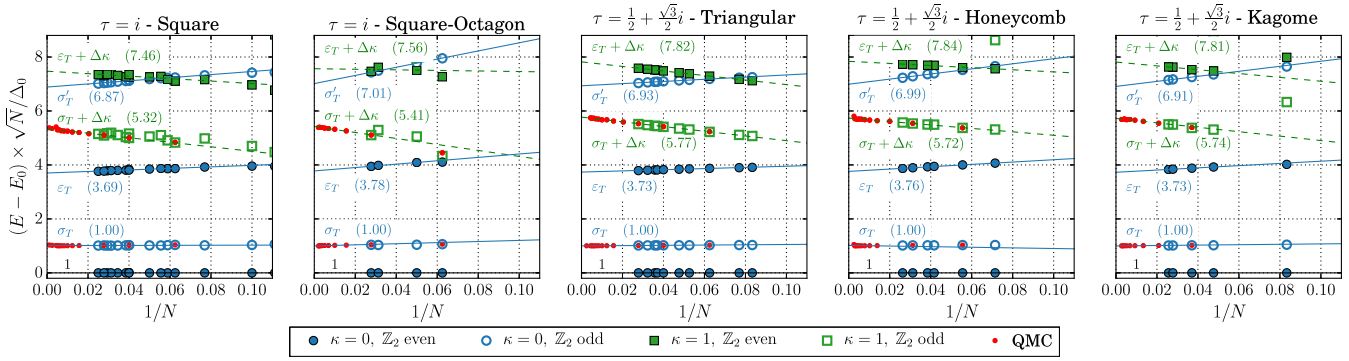

FIG. 2. Normalized low-energy torus spectrum for the Ising QFT for the modular parameters $\tau = i$ and $\tau = 1/2 + \sqrt{3}/2i$ obtained with ED (large symbols) and QMC simulations (small red filled circles). Filled (empty) symbols denote $\mathbb{Z}_2$ even (odd) levels. Linear fits in $1/N$ for levels with $\kappa = 0$ ($\kappa = 1$) are shown by blue solid (green dashed) lines (cf. color coding in Fig. 1) and the values of the fields after extrapolation to the thermodynamic limit $1/N \to 0$ are given in parentheses. The normalization constant Δ_0 is chosen such that the first $\mathbb{Z}_2$ odd level extrapolates to one. We observe a universal torus spectrum for the lattices with the same type of IR cutoff (same τ).

symmetries are preserved during the calculation and no extra length scales are introduced.

Our approach to the critical theory in a finite volume originated from Lüscher [40], and was extended to deal with finite size criticality in classical systems by others [33,41]. The key observation is that the zero mode of the field generates incurable infrared divergences in perturbation theory, so it must be separated and treated nonperturbatively. In the context of the finite-size spectrum, this can be understood from Eq. (2) by noticing that the Gaussian theory at $s = 0$ does not contain any potential term for the zero mode, giving a continuous spectrum, whereas any finite u will confine the zero mode producing a discrete spectrum. Therefore, the correct perturbative approach is to treat the momentum of the zero mode at the same order as its interactions.

By splitting the fields in Eq. (2) and proper normalization of the zero-mode terms, the Hamiltonian can be decomposed into a quadratic part $\mathcal{H}_0$ describing the Fock spectrum of the finite-momentum modes, and an interaction part V containing all zero-mode contributions and nonlinearities.

At zeroth order, our states are given by finite momentum Fock states multiplied by arbitrary functionals of the zero mode, so these states are infinitely degenerate. We then derive an effective Hamiltonian within each degenerate subspace using a perturbation method due to Bloch [42]. This effective Hamiltonian acts in a degenerate subspace, but its eigenvalues correspond to the exact eigenvalues of the original Hamiltonian to desired order. It turns out, that the effective Hamiltonians take the form of a strongly coupled oscillator with coefficients depending on the degenerate subspaces. The coefficients of the more complicated expansion for the energy levels (expansion in $\epsilon^{1/3}$) can be found in Ref. [34]. In addition, the effective Hamiltonian will couple different Fock states with the same energy and momentum whenever possible, leading to off-diagonal terms. These off-diagonal terms were computed numerically from the unperturbed wave function. Further details about the ϵ-expansion approach can be found in the Supplemental Material [32].

In Fig. 3 we show the universal torus spectrum obtained from ϵ expansion for the two choices of τ and compare it to numerical results from ED and QMC computations [32(d)] normalized by the speed of light c [32(e),43]. We observe a remarkable agreement between the two different methods. This further illustrates the interpretation of the torus spectra as a universal fingerprint of the critical field theory and their accessability from numerical finite lattice simulations. The larger discrepancies between numerical and ϵ-expansion data for some higher levels in the spectrum may result from the extrapolation to the thermodynamic limit using only ED data with strong finite-size effects, especially for $\kappa > 0$ [44].

$(2+1)$D *Ising* universality class.*—In this section we are investigating the confinement transition of a $\mathbb{Z}_2$ spin

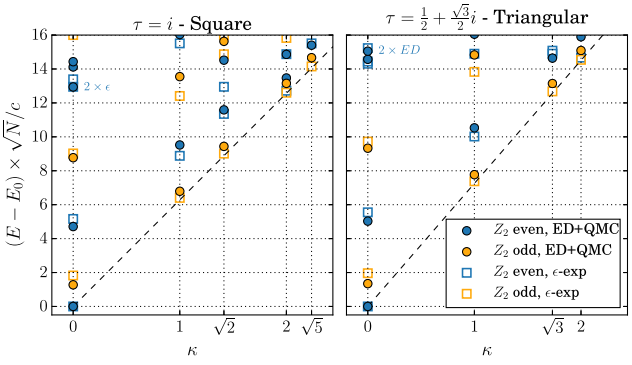

FIG. 3. Universal torus spectra for the Ising QFT for the modular parameters $\tau = i$ (left panel) and $\tau = 1/2 + \sqrt{3}/2i$ (right panel). Full symbols denote numerical results obtained by ED + QMC (the lowest Z_2 odd levels), while empty symbols denote the ϵ-expansion results. The dashed line shows a dispersion according to the speed of light.

liquid. Such a topological quantum phase transition is characterized by the lack of any local order parameters. $\mathbb{Z}_2$ spin liquids are characterized by the presence of two bosons, the e and m particles. These fractionalized particles can only be created in pairs and obey mutual anyonic statistics. The confinement transition can then be driven by condensing either the e or the m particles. Without loss of generality, we will consider the condensation of the m particles and call it's corresponding field ϕ. The critical theory turns out to be that of Ising*: ϕ can only be created in pairs, so the effective Lagrangian must be even in a real field ϕ, implying we should only include $\mathbb{Z}_2$ even states in a critical Ising theory. In addition, ϕ and $-\phi$ are physically indistinguishable, and so both periodic and antiperiodic boundary conditions have to be considered. We emphasize that this mapping is independent of any specific microscopic lattice model and should hold generically between universal theories and their topological counterparts.

As a microscopic model illustrating this transition, we study the critical energy spectrum of the toric code Hamiltonian perturbed by a longitudinal field [45–49]:

$$H_{\mathrm{TC}} = -J\sum_s A_s - J\sum_p B_p - h\sum_i \sigma_i^x$$
$$A_s = \prod_{i\in s}\sigma_i^x, \qquad B_p = \prod_{i\in p}\sigma_i^z. \tag{3}$$

The σ_i describe $S = 1/2$ spins on the $2N$ edges of a square lattice, p denotes a plaquette, and s a star on the lattice. All A_s and B_p commute with each other and so the model can be solved analytically for $h = 0$ by setting all $A_s = 1$ and all $B_p = 1$ [50]. On a torus, the ground state manifold is, however, fourfold degenerate and can be characterized by the eigenvalues ± 1 of Wilson loops winding around the torus. An e (m) particle is described by setting $A_s = -1$ ($B_p = -1$) on a star (plaquette). The longitudinal field introduces a dispersion for the m particles which finally condense and drive the phase transition at $h = h_c$ by confinement of the e particles [29–31,45].

The above considerations regarding the relationship between Ising and Ising* quantum field theory (QFT) can be made very explicit for the toric code. The toric code Eq. (3) in the sector without e particles ($A_s = 1$) can be exactly mapped to an even TFI model on the dual square lattice with N sites, where only the even spin-flip sector is present [45,51,52]. The ground state manifold, described by the eigenvalues of the Wilson loops, maps to both, periodic and antiperiodic boundary conditions of the Ising model [32(f)]. In the following we will make use of this mapping to compute the finite-size torus spectrum of the Ising* transition for $\tau = i$ using ED.

In the left part of Fig. 4 we present the low-energy finite-size spectrum of the Ising* transition obtained with ED simulations. The spectrum is rescaled with the same factor Δ_0 as in Fig. 2 such that they can be easily compared. The

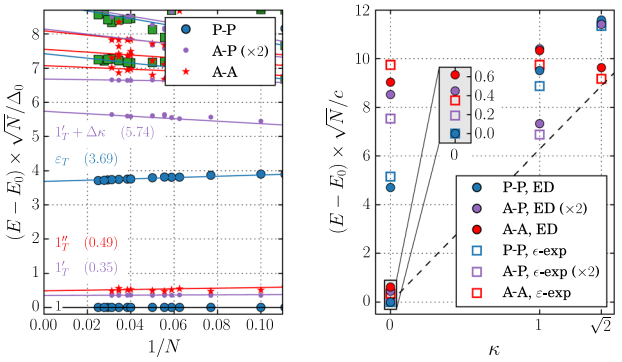

FIG. 4. Universal torus spectra for the Ising* QFT and the modular parameter $\tau = i$. The labels A-P etc. denote the boundary conditions along the two directions of the torus, where P (A) means periodic (antiperiodic). Left: Normalized low-energy spectrum from ED with the same normalization constant Δ_0 as in Fig. 2. The levels in the P-P sector are the $\varepsilon_T(+\Delta\kappa)$ levels from the TFI spectrum. A very remarkable feature is the presence of the four very low-lying levels which govern the fourfold degenerate ground state manifold in the deconfined phase. See Fig. 2 for further details. Right: Full symbols denote numerical results obtained by ED, while empty symbols denote ϵ-expansion results. The dashed line shows a dispersion with the speed of light. The inset is an enlargement of the four lowest levels. See Fig. 3 for further details.

relationship between the critical Ising and Ising* theories results in the fact that the levels called $\varepsilon_T(+\Delta\kappa)$ in Fig. 2 are identically present in the Ising* spectrum (c.f. P-P levels in Fig. 4). The most remarkable feature, however, is the presence of very low-lying levels in the spectrum. They arise from the ground state manifold in the spin-liquid phase, where their splitting exponentially scales to zero with L. At criticality they, however, scale as $1/\sqrt{N}$ as the entire low-energy spectrum. The small relative splitting of the four lowest levels is surprisingly small. The right panel of Fig. 4 shows a comparison of the universal torus spectrum for an Ising* transition obtained with ED and ϵ expansion similar to Fig. 3 [32(g)]. An enlargement of the conspicuous low-energy levels is shown in the inset. Again we observe a decent agreement of the different methods.

Conclusions.—We have computed the universal torus energy spectrum for the Ising and Ising* transitions in $(2+1)$D providing a characteristic fingerprint of the corresponding conformal field theories and have highlighted the implications of a neighboring $\mathbb{Z}_2$ spin liquid on the torus spectrum. Additionally, we have highlighted a phenomenological picture based on the quantum numbers of the individual energy levels which shows a structure qualitatively similar to the operator content of the field theory in flat space. Using the numerical and analytical technology presented in this Letter it will be possible to inspect and chart the characteristic spectrum of more complex quantum critical points, such as $O(N)$ Wilson-Fisher fixed points, Gross-Neveu-Yukawa type phase transitions in interacting

Dirac fermion models [53,54], or designer Hamiltonians displaying deconfined criticality [2].

A. M. L. thanks R. C. Brower, J. L. Cardy, and A. W. Sandvik for discussions. L.-P. H. and M. S. acknowledge support through the Austrian Science Fund SFB FoQus (F-4018). S. W. and S. S. are supported by the U.S. NSF under Grant No. DMR-1360789. We thank A. Wietek for his help on computing large-scale ED results. The computational results presented have been achieved in part using the Vienna Scientific Cluster (VSC). This work was supported by the Austrian Ministry of Science BMWF as part of the UniInfrastrukturprogramm of the Focal Point Scientific Computing at the University of Innsbruck. Research at Perimeter Institute is supported by the Government of Canada through Industry Canada and by the Province of Ontario through the Ministry of Research and Innovation. This research was supported in part by the National Science Foundation under Grant No. NSF PHY11-25915.

[1] T. Senthil, A. Vishwanath, L. Balents, S. Sachdev, and M. P. A. Fisher, Deconfined Quantum Critical Points, Science **303**, 1490 (2004).

[2] A. W. Sandvik, Evidence for Deconfined Quantum Criticality in a Two-Dimensional Heisenberg Model with Four-Spin Interactions, Phys. Rev. Lett. **98**, 227202 (2007).

[3] S. El-Showk, M. F. Paulos, D. Poland, S. Rychkov, D. Simmons-Duffin, and A. Vichi, Solving the 3D Ising model with the conformal bootstrap, Phys. Rev. D **86**, 025022 (2012); Solving the 3d Ising model with the conformal bootstrap II. c-minimization and precise critical exponents, J. Stat. Phys. **157**, 869 (2014).

[4] C. Holzhey, F. Larsen, and F. Wilczek, Geometric and renormalized entropy in conformal field theory, Nucl. Phys. **B424**, 443 (1994).

[5] P. Calabrese and J. Cardy, Entanglement entropy and quantum field theory, J. Stat. Mech. Theor. Exp. P06002 (2004).

[6] A. M. Läuchli, Operator content of real-space entanglement spectra at conformal critical points, arXiv:1303.0741.

[7] A. B. Kallin, K. Hyatt, R. R. P. Singh, and R. G. Melko, Entanglement at a Two-Dimensional Quantum Critical Point: A Numerical Linked-Cluster Expansion Study, Phys. Rev. Lett. **110**, 135702 (2013).

[8] P. Bueno, R. C. Myers, and W. Witczak-Krempa, Universality of Corner Entanglement in Conformal Field Theories, Phys. Rev. Lett. **115**, 021602 (2015).

[9] In a corresponding classical statistical mechanics language, we are discussing the spectrum of the logarithm of the transfer matrix in the limit of an infinitely long square (or hexagonal) rod (c.f. left part of Fig. 1). The transfer matrix acts along the infinite rod direction.

[10] J. L. Cardy, Conformal invariance and universality in finite-size scaling, J. Phys. A **17**, L385 (1984).

[11] A. Feiguin, S. Trebst, A. W. W. Ludwig, M. Troyer, A. Kitaev, Z. Wang, and M. H. Freedman, Interacting Anyons in Topological Quantum Liquids: The Golden Chain, Phys. Rev. Lett. **98**, 160409 (2007).

[12] H. Suwa and S. Todo, Generalized Moment Method for Gap Estimation and Quantum Monte Carlo Level Spectroscopy, Phys. Rev. Lett. **115**, 080601 (2015).

[13] J. L. Cardy, Universal amplitudes in finite-size scaling: generalisation to arbitrary dimensionality, J. Phys. A **18**, L757 (1985).

[14] F. C. Alcaraz and H. J. Herrmann, Numerical difficulties in obtaining 3D critical exponents from Platonic solids, J. Phys. A **20**, 5735 (1987).

[15] M. Weigel and W. Janke, Universal amplitude-exponent relation for the Ising model on sphere-like lattices, Europhys. Lett. **51**, 578 (2000).

[16] Y. Deng and H. W. J. Blöte, Conformal Invariance of the Ising Model in Three Dimensions, Phys. Rev. Lett. **88**, 190602 (2002).

[17] R. C. Brower, G. T. Fleming, and H. Neuberger, Lattice radial quantization: 3D Ising, Phys. Lett. B **721**, 299 (2013).

[18] R. C. Brower, G. Fleming, A. Gasbarro, T. Raben, C.-I. Tan, and E. Weinberg, Quantum Finite Elements for Lattice Field Theory, arXiv:1601.01367.

[19] M. Henningson and N. Wyllard, Low-energy spectrum of $N = 4$ super-Yang-Mills on T^3: Flat connections, bound states at threshold, and S-duality, J. High Energy Phys. 06 (2007) 001.

[20] M. Henningson and F. Ohlsson, BPS partition functions in $N = 4$ Yang-Mills theory on T^4, J. High Energy Phys. 03 (2011) 145.

[21] S. Banerjee, S. Hellerman, J. Maltz, and S. H. Shenker, Light states in Chern-Simons theory coupled to fundamental matter, J. High Energy Phys. 03 (2013) 097.

[22] M. G. Pérez, A. González-Arroyo, and M. Okawa, Spatial volume dependence for $2 + 1$ dimensional SU(N) Yang-Mills theory, J. High Energy Phys. 09 (2013) 003.

[23] E. Shaghoulian, Modular forms and a generalized Cardy formula in higher dimensions, Phys. Rev. D **93**, 126005 (2016).

[24] M. Henkel, Universal ratios of scaling amplitudes in the Hamiltonian limit of the 3D Ising model, J. Phys. A **19**, L247 (1986); Finite size scaling and universality in the $(2 + 1)$D Ising model, J. Phys. A **20**, 3969 (1987).

[25] J. L. Cardy, Anisotropic corrections to correlation functions in finite-size systems, Nucl. Phys. **B290**, 355 (1987).

[26] C. J. Hamer, Finite-size scaling in the $(2 + 1)$D Ising model, J. Phys. A **16**, 1257 (1983); The $(2 + 1)$D Ising model on a triangular lattice, J. Phys. A **19**, 423 (1986); Finite-size scaling in the transverse Ising model on a square lattice, J. Phys. A **33**, 6683 (2000).

[27] Y. Nishiyama, Bound-state energy of the three-dimensional Ising model in the broken-symmetry phase: Suppressed finite-size corrections, Phys. Rev. E **77**, 051112 (2008).

[28] S. Dusuel, M. Kamfor, K. P. Schmidt, R. Thomale, and J. Vidal, Bound states in two-dimensional spin systems near

the Ising limit: A quantum finite-lattice study, Phys. Rev. B **81**, 064412 (2010).
[29] R. A. Jalabert and S. Sachdev, Spontaneous alignment of frustrated bonds in an anisotropic, three-dimensional Ising model, Phys. Rev. B **44**, 686 (1991).
[30] S. Sachdev and M. Vojta, Translational symmetry breaking in two-dimensional antiferromagnets and superconductors, J. Phys. Soc. Jpn. Suppl. B **69**, 1 (1999).
[31] T. Senthil and M. P. A. Fisher, Z_2 gauge theory of electron fractionalization in strongly correlated systems, Phys. Rev. B **62**, 7850 (2000).
[32] See Supplemental Material at http://link.aps.org/supplemental/10.1103/PhysRevLett.117.210401 for (a) a definition of the Archimedian lattices, (b) motivation of this $1/N$ finite-size extrapolation approach, (c) further details about the used gap estimation procedure for QMC simulations, (d) a listing of the complete low-energy torus spectra for the Ising transition from numerics and ϵ-expansion, (e) the details on the determination of c, which includes Refs. [26,37], (f) a detailed discussion of the mapping, and (g) a listing of the complete low-energy torus spectra for the Ising* transition from numerics and ϵ expansion, which includes Refs. [33–37].
[33] J. Rudnick, H. Guo, and D. Jasnow, Finite-size scaling and the renormalization group, J. Stat. Phys. **41**, 353 (1985).
[34] L. Skála, J. Cízek, and J. Zamastil, Strong coupling perturbation expansions for anharmonic oscillators. Numerical results, J. Phys. A **32**, 5715 (1999).
[35] D. J. Klein, Degenerate perturbation theory, J. Chem. Phys. **61**, 786 (1974).
[36] J. Zinn-Justin, *Quantum Field Theory and Critical Phenomena*, International Series of Monographs on Physics (Clarendon Press, Oxford, 2002).
[37] S. Whitsitt and S. Sachdev, Transition from the $\mathbb{Z}_2$ spin liquid to antiferromagnetic order: Spectrum on the torus, Phys. Rev. B **94**, 085134 (2016).
[38] H. W. J. Blöte and Y. Deng, Cluster Monte Carlo simulation of the transverse Ising model, Phys. Rev. E **66**, 066110 (2002).
[39] We have computed the critical point for the square-octagon lattice as $(h/J)_c = 2.087(7)$ using a continous-time QMC algorithm similar to that of Ref. [38].
[40] M. Lüscher, A new method to compute the spectrum of low-lying states in massless asymptotically free field theories, Phys. Lett. B **118**, 391 (1982).
[41] E. Brézin and J. Zinn-Justin, Finite size effects in phase transitions, Nucl. Phys. **B257**, 867 (1985).
[42] C. Bloch, Sur la théorie des perturbations des états liés, Nucl. Phys. **6**, 329 (1958).
[43] A. Sen, H. Suwa, and A. W. Sandvik, Velocity of excitations in ordered, disordered, and critical antiferromagnets, Phys. Rev. B **92**, 195145 (2015).
[44] For further studies it is worth noticing that ϵ expansion tends to overestimate the $\kappa = 0$ levels while levels with $\kappa > 0$ are commonly underestimated.
[45] S. Trebst, P. Werner, M. Troyer, K. Shtengel, and C. Nayak, Breakdown of a Topological Phase: Quantum Phase Transition in a Loop Gas Model with Tension, Phys. Rev. Lett. **98**, 070602 (2007).
[46] J. Vidal, S. Dusuel, and K. P. Schmidt, Low-energy effective theory of the toric code model in a parallel magnetic field, Phys. Rev. B **79**, 033109 (2009).
[47] I. S. Tupitsyn, A. Kitaev, N. V. Prokof'ev, and P. C. E. Stamp, Topological multicritical point in the phase diagram of the toric code model and three-dimensional lattice gauge Higgs model, Phys. Rev. B **82**, 085114 (2010).
[48] S. Dusuel, M. Kamfor, R. Orús, K. P. Schmidt, and J. Vidal, Robustness of a Perturbed Topological Phase, Phys. Rev. Lett. **106**, 107203 (2011).
[49] F. Wu, Y. Deng, and N. Prokof'ev, Phase diagram of the toric code model in a parallel magnetic field, Phys. Rev. B **85**, 195104 (2012).
[50] A. Y. Kitaev, Fault-tolerant quantum computation by anyons, Ann. Phys. (Amsterdam) **303**, 2 (2003).
[51] A. Hamma and D. A. Lidar, Adiabatic Preparation of Topological Order, Phys. Rev. Lett. **100**, 030502 (2008).
[52] *Understanding Quantum Phase Transitions*, edited by L. Carr, Condensed Matter Physics, Vol. 20103812 (CRC Press, Boca Raton, Florida, 2010).
[53] L. Wang, P. Corboz, and M. Troyer, Fermionic quantum critical point of spinless fermions on a honeycomb lattice, New J. Phys. **16**, 103008 (2014).
[54] Z.-X. Li, Y.-F. Jiang, and H. Yao, Fermion-sign-free Majarana-quantum-Monte-Carlo studies of quantum critical phenomena of Dirac fermions in two dimensions, New J. Phys. **17**, 085003 (2015).